DYNAMICS OF SUSPENSIONS IN SHEAR FLOWS

By James W. Daily,* *Member*

(Presented as one of the John R. Freeman Lectures on Fundamental Hydraulic Processes in Water Resources Engineering, Boston Society of Civil Engineers, Fall, 1963.)

Introduction

Interest in suspensions in shear flows stems from many sources. The transport of sediment in streams and of various materials in pipes and ducts are the first that come to mind. In the myriad of applications of these basic processes, questions arise as to the flow resistance, the distribution of the particle material in the stream and the effects of the particles on the transfer of momentum and the processes of diffusion and mixing. It has not been possible to answer these questions by applying the hydrodynamic laws which hold for common fluids. Suspensions display important departures from such laws which have lead to many investigations over a long period of years. This article will attempt to summarize some of the significant findings.

The behavior of a suspension of particles may be viewed in two ways. One is to examine its overall or "bulk flow" behavior as though the two-phase medium had the properties of a homogeneous substance. The second is to recognize a suspension as composed of two distinct phases and to examine the interactions between the two phases and the confining boundaries.

The former is interesting because the overall behavior of a flowing suspension may be non-Newtonian although the suspending fluid is Newtonian. As a consequence, some of the models used to define the rheological behavior of non-Newtonian fluids have been applied to suspensions. The second is the more significant and yet more difficult. It involves study of the Newtonian hydrodynamics of immersed particles in a highly complicated situation. Rigorous analysis has not been possible but deductions from direct and indirect experimental observations have lead to some understanding of the mechanics involved. The present paper is primarily a discussion of the results of examinations from the second point of view but will be introduced by a brief descrip-

* Professor of Civil Engineering, Massachusetts Institute of Technology, Cambridge 39, Massachusetts.

tion of the simplest rheological flow models that have their analogies in suspension behavior.

Some Rheological Models

Rheology is the study of the relation between shear stress and fluid deformation. Ordinarily we deal with fluids following the Newtonian relation

$$\tau = \mu \frac{du}{dy} \tag{1}$$

where μ is the dynamic viscosity of the fluid and is constant, τ the shear stress and du/dy the velocity gradient. This linear relation is merely the most simple one. Many fluids follow other relations which are generally classified as indicated in Fig. 1. One group is time-independent and includes the Newtonian fluids. A second group is time-dependent. The latter may stiffen under shear with time (rheopactic) or may relax

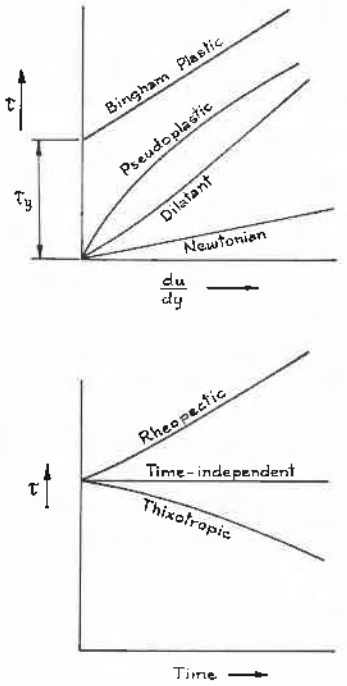

FIG. 1.—TYPES OF RHEOLOGICAL BEHAVIOR

with time (thixotropic). Some fluids require a definite yield stress before flow will take place.

The time-independent behaviors are represented by mathematical models. The Newtonian model of Eq. (1) is the simplest. Two more complex representations are the Bingham plastic model and the power law model. The Bingham plastic relation is

$$\tau = \tau_y + \mu_s \frac{du}{dy} \tag{2}$$

where τ_y is the yield stress and μ_s is the slope viscosity. For $\tau_y = 0$ this reduces to the Newtonian case. The power law model is

$$\tau = K \left(\frac{du}{dy} \right)^n \tag{3}$$

which is the equation of a straight line of slope n and intercept K in a log τ versus log du/dy diagram. This equation is devised to model either the pseudoplastic or dilatant behavior illustrated in Fig. 1. The exponent n is dimensionless and < 1.0 for the pseudoplastic, > 1.0 for the dilatant; K has dimensions which depend on the value of n.

At the boundary Eq. (3) becomes

$$\tau_o = \left[K \left(\frac{du}{dy} \right)^n \right]_{wall} \tag{3a}$$

In some cases du/dy at the wall is proportional to the ratio of the maximum or mean velocity to the pipe diameter. For Newtonian fluids du/dy at the wall $\propto 8V/D$. Using this we can express the wall shear as

$$\tau_o = K' \left(\frac{8V}{D} \right)^{n'} \tag{4}$$

where K′ and n′ can be related to K and n.

Eqs. (1), (2) and (3) correspond to the following velocity distributions and shear stress relations:

For Newtonian flow:

$$u = \frac{1}{4\mu} \frac{\Delta P}{L} (R^2 - r^2) \tag{5}$$

$$\tau_o = \mu \frac{8V}{D} \tag{6}$$

For Bingham plastic flow:

$$u = \frac{1}{4\mu_s}\left[\frac{\Delta P}{L}(R^2 - r^2) - \tau_y(R - r)\right] \tag{7}$$

(valid for the portion of the cross-section where $\tau > \tau_y$, i.e., where $r > R_p = \tau_y 2L/\Delta P$, R_p being the plug radius).

Eq. (7) gives the profile shown in Fig. 2 which consists of an annular sheared layer and a central unsheared core. Under some circumstances suspensions form plugs in the central portion of pipes over which the

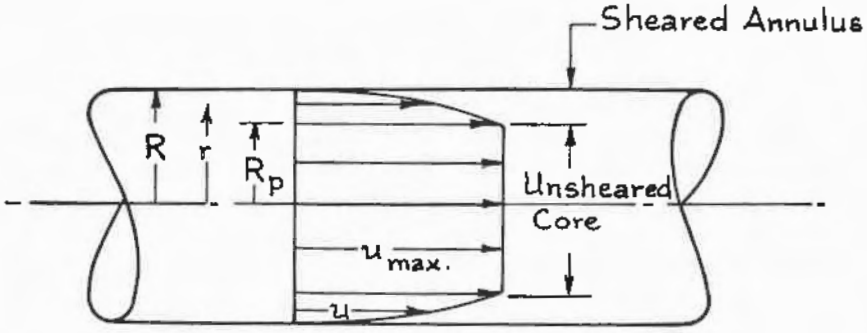

FIG. 2.—BINGHAM PLASTIC VELOCITY PROFILE—A MODEL FOR PLUG FLOW

velocity is essentially constant and which are surrounded by a highly sheared layer of suspension-free fluid. The Bingham plastic model has been used to describe such cases. The Bingham plastic wall shear is

$$\tau_o = \frac{\mu_s}{1 - 4/3(t_y/t_o) + (1/3)(\tau_y/\tau_o)^4}\,\frac{8V}{D} \tag{8}$$

For pseudoplastic or dilatant flow

$$u = \frac{n}{n+1}\,\frac{1}{K^{n/1}}\left(\frac{\Delta P}{2L}\right)^{1/n}(R^{(1/n)+1} - r^{(1/n)+1}) \tag{9}$$

(which gives a profile blunter than the corresponding Newtonian if $n < 1$, and sharper if $n > 1$),

$$\tau_o = K\left(\frac{1+3n}{4n}\right)^n\left(\frac{8V}{D}\right)^n \tag{10}$$

Expressing the friction factor as

$$f = \frac{8\tau_o}{\rho V^2} \tag{11}$$

we see that the Bingham plastic model, like the Newtonian, gives

$$f\alpha \frac{1}{VD} \tag{12}$$

This is a "laminar flow" model and we conclude that, if turbulence does not occur, very low friction factors are possible as V is increased. The power law model also gives a reduction in f with increasing V so long as $n \leqslant 2$. In principle, the power law model has more generality in that by adjusting n and K both laminar and turbulent behavior might be described.

These models are useful as a framework for classifying types of behavior and, to a limited extent, in aiding correlation of behavior data. None can serve with generality, however. Basically they assume the fluid to be homogeneous in its properties. Suspensions are multiphase systems and concentration differences, and even phase separation, can occur in different regions of a stream. Consequently the mechanism of momentum transfer may vary across the shear field. (The Bingham plastic model gives one type of variation by limiting deformation to zones of stress higher than a yield stress.) We shall see in subsequent discussions that such variations are important.

Effective Viscosity

There is another concept which falls into the category of rheology. Instead of a model such as one of the previous, shear can be represented by Eq. (1) with the coefficient being an *effective viscosity* instead of the Newtonian value. For suspensions this amounts to considering the multiphase system as an equivalent homogeneous fluid. Albert Einstein (7) first showed analytically that additional energy dissipation results in *laminar* shear flow when particles are present (this was the subject of his doctoral dissertation). In other words, the effective viscosity is greater than the Newtonian viscosity of the suspending medium. He obtained for small concentrations the relative effect as

$$\eta = \frac{\nu_e}{\nu} = (1 + 2.5\,C') \tag{13}$$

where

ν_e = effective viscosity
ν = Newtonian viscosity of suspending medium
C' = volume concentration
= vol. of solids/(vol. solids + vol. fluid)

A subsequent expression for finite concentrations is that of Eilers (8) found experimentally to be

$$\eta = \left\{1 + \frac{2.5\,C'}{2(1 - 1.35\,C')}\right\}^2 \tag{14}$$

These and many other analytical and empirical results have their limitations: First, each analytical result depends on the particular physical model assumed, e.g., arrangement of particles in space. Second, the empirical results depend on the wall effects and hence on the relative size of the particle to the shear field dimensions. In addition, of course, all results are for laminar flow and do not describe the effective viscosity in the turbulent range. In many cases the effective viscosity has been found a function of the shear rate, i.e., the gradient $d\bar{u}/dy$. This is what would be indicated by a material obeying the power law model completely. The above equations indicate no effect of shear rate on effective viscosity of solid particle suspensions, but it is not clear that this is generally true.

Suspensions of Finite Solid Particles

Turning now to suspensions of finite solid particles, we will consider three cases. First, rigid particles of high specific gravity. Second, highly flexible particles of low specific gravity. Third, rigid particles of nearly neutral buoyancy.

Experiments with Sediments

Entrained sediments in natural streams probably were the first suspensions to be studied in detail. Natural sand and silt particles have the characteristics of a large specific gravity (2.65 for quartz), rigid irregular shapes and an assortment of sizes. Gravity causes settling so only for flows above some incipient motion condition will particles be lifted into suspension (see lecture by J. F. Kennedy in this series published in Oct. 1965 *Journal*). With the particles entrained, only turbu-

lence will keep them in suspension against the gravity effect.

The role of turbulence in maintaining the suspension is based on the idea that the rate of vertical turbulent mixing is in balance with the rate of "fall out" of particles, thus

$$G = w\,c = -\varepsilon_s \frac{dc}{dy} \tag{15}$$

where

w = particle fall velocity
$c = c(y)$ = particle concentration in mass/vol.
$\varepsilon_s(y)$ = sediment vertical transfer coefficient
y = vertical direction (approximately normal to flow direction in an open channel).

This is analogous to the shear stress equation (which gives the momentum transfer), namely

$$\tau = \rho\,\varepsilon_m \frac{d\bar{u}}{dy} \tag{16}$$

where

$\tau = \tau(y)$ = shear stress
ρ = fluid density in mass/vol.
$\varepsilon_m(y)$ = momentum transfer coefficient
$\bar{u} = \bar{u}(y)$ = local mean velocity.

Assuming $\varepsilon_s(y) = \varepsilon_m(y)$ and τ is a linear function of y, Ippen integrated Eq. (15) using the Kármán-Prandtl velocity defect equation

$$\frac{\bar{u}_{max} - \bar{u}}{u_*} = \frac{1}{k} \ln \frac{d}{y} \tag{17}$$

where

$\bar{u}_{max} - \bar{u}$ = local mean velocity defect
$u_* = \sqrt{\tau_o/\rho}$ = friction velocity
k = Kármán's "universal" constant
d = depth of flow

to obtain

$$\frac{c}{c_a} = \left(\frac{a - y}{y} \frac{a}{d - a} \right)^z \tag{18}$$

where

c_a = concentration at an arbitrary reference level y = a

$$z = \frac{w}{k\, u_*}.$$

The first definitive study of the relation between turbulently suspended sediment load, sediment distribution, flow velocity distribution and channel slope and flow rate was made by Vanoni (1). He experimented in a two-dimensional open channel with fine sediments having

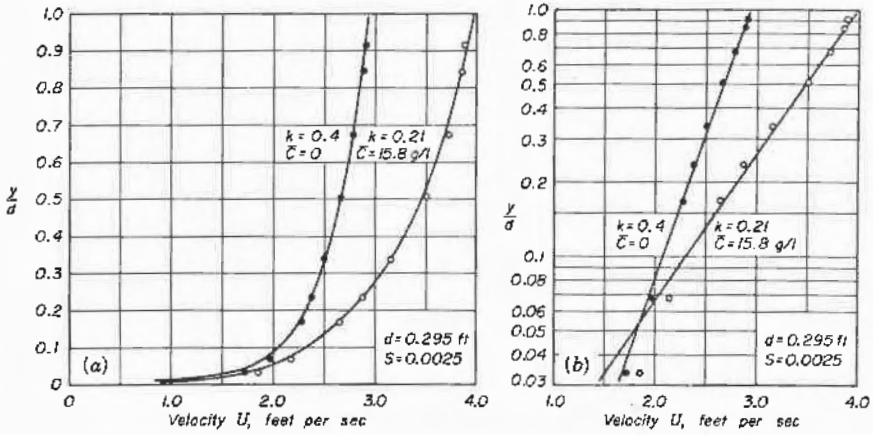

FIG. 3.—VELOCITY PROFILES FOR THE SAME CHANNEL SLOPE AND DEPTH—OPEN CHANNEL WITH FINE SEDIMENT.

diameters of 0.0147, 0.0120, and 0.0091 centimeters. To eliminate the effects of variable roughness encountered with erodible beds, he established a fixed roughness by cementing relatively large sand grains to a plain bottom. The sediment concentrations and flow velocities were such that the sand was essentially all suspended with negligible bed load. He found that for the same channel slope and depth of flow an increased volume flow rate when sediment was added. This is shown by the velocity profiles in Fig. 3 where it can be seen that the integral of the sharper profile with sediment exceeds that of the water profile. This means that the flow resistance is reduced or that the Chezy "C" is increased. It can be expressed as a reduction in the effective value of n in Manning's formula or a reduction in the friction factor f since

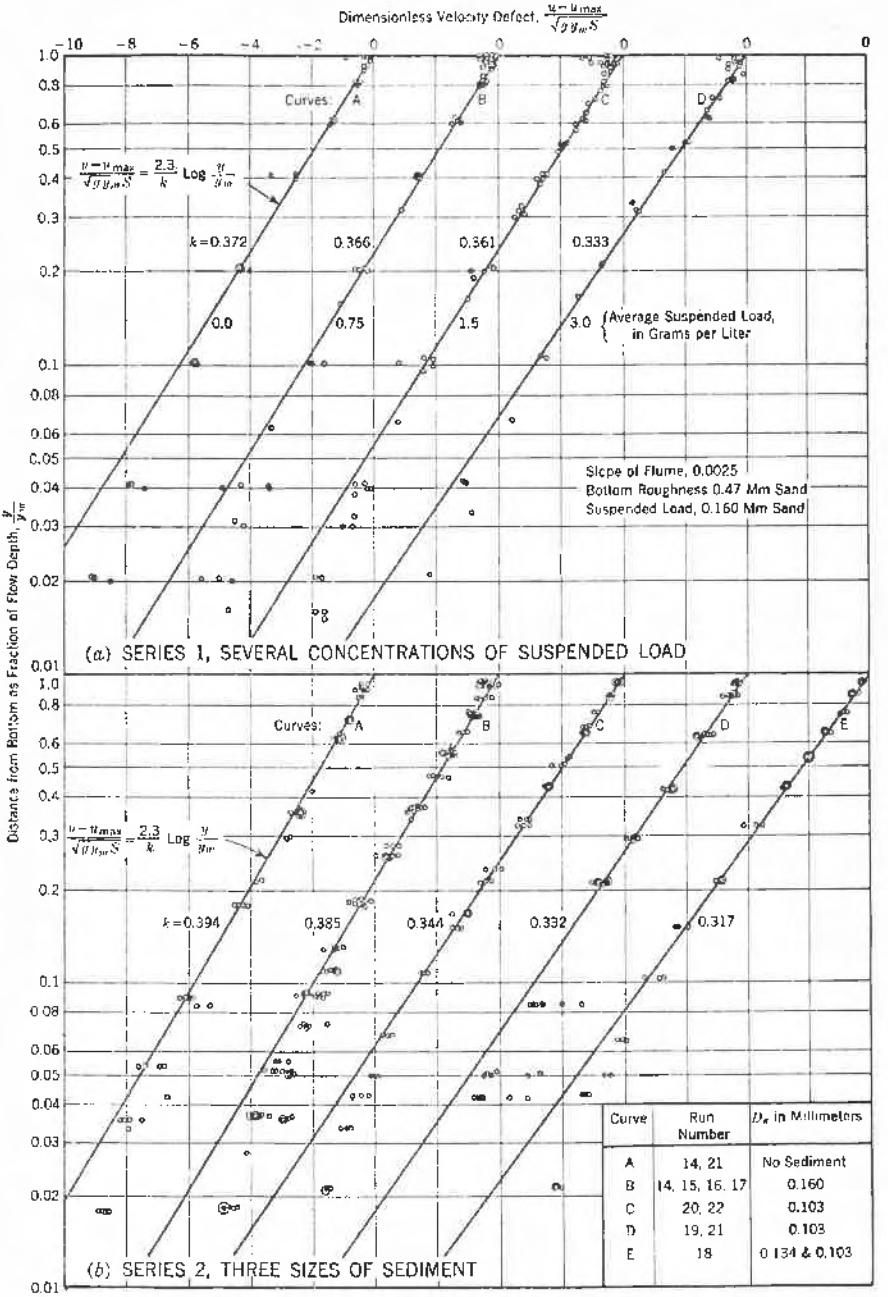

FIG. 4.—DIMENSIONLESS VELOCITY DEFECT—OPEN CHANNEL WITH FINE SEDIMENT (REF. 1).

$$\text{Chezy } C = \frac{1.49\, R^{1/6}}{n} = \sqrt{\frac{8g}{f}} \qquad (19)$$

where R is the hydraulic radius. As seen in Fig. 4, Vanoni found that with sediment the velocity profile in the upper portion of the flow could be represented by the Kármán-Prandtl logarithmic equation. Furthermore, the results showed that k decreased with increased concentration as shown in Fig. 4. The constant k is related to the turbulence structure

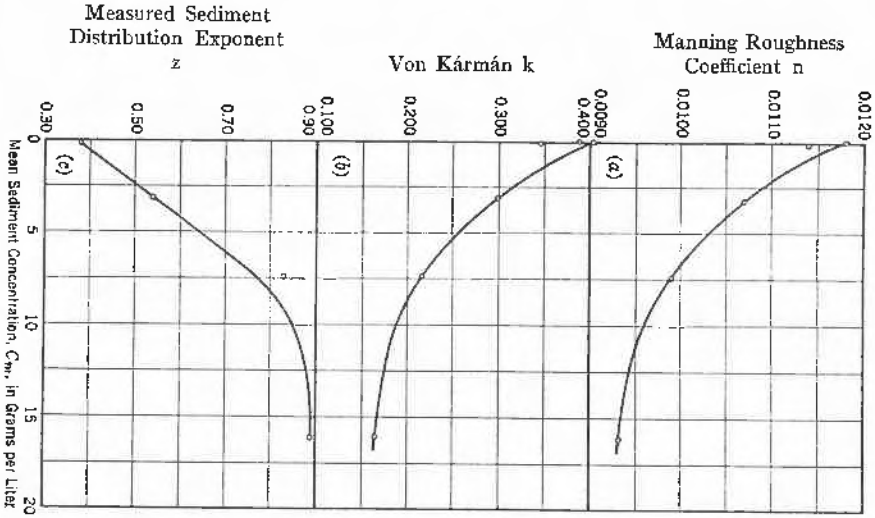

FIG. 5.—SUSPENDED LOAD CONCENTRATION EFFECTS IN OPEN CHANNEL—FINE SEDIMENT (REF. 1).

for Newtonian homogeneous fluids. A reduced value corresponds to a sharper velocity profile and lower shear stress. Since sediment gave this result, it was interpreted as signifying a reduced turbulence. It was reasoned that the work of keeping the sediment in suspension suppressed the vertical turbulence velocity component.

This departure of the friction factor from the water value is a non-Newtonian behavior. It is an interesting one because the theoretical effect of particles in a laminar shear flow would be an *increase* in effective viscosity (as already noted). Shear reduction would seem to correspond to a *decrease* in the effective viscosity. There is a condition of prime importance to consider, however. The suspension at the wall

cannot have the same properties and effects as the same suspension away from a solid boundary. Both particle concentration and particle interactions are affected.

Vanoni found that Eq. (18) was of the correct form to describe sediment distribution but the theoretical exponent z differed from the experimental value z_1. He also found that the turbulent transfer coefficients ε_m and ε_s were not identically the same, although no consistent trend could be observed. Since the derivation of Eq. (18) assumes identity, this may have some bearing on the deviation of the exponent from its theoretical value.

All these findings are summarized in Fig. 5 where their variations are shown as a function of the concentration.

Ismail (2) employed a closed rectangular channel with horizontal smooth top and bottom walls and repeated Vanoni's experiments using 0.10 mm and 0.16 mm sands. Ismail's concentrations were such that bed loads formed at low Reynolds numbers with large increases in the friction factor f over the clear water value. These results are shown in Fig. 6. At high Reynolds numbers f dropped and, within the experimental accuracy, seemed to approach the clear water values (labelled erroneously as Eq. (12) in the figure). Ismail also found sharper velocity profiles and a reduction in the Kármán k with sediment additions. However, his velocity profiles for the suspensions were asymmetric and the upper portion (towards the "ceiling") was fuller, with higher k, than the lower portion. His results give the sediment vertical transfer coefficient higher than the momentum transfer coefficient. He found $\varepsilon_s = 1.5\ \varepsilon_m$ for 0.10 mm sand and $\varepsilon_s = 1.3\ \varepsilon_m$ for 0.16 mm sand.

Except for very high concentrations or low velocities the behavior of the dense sediment suspensions does not seem to be described by one of the rheological models cited. First, of course, the models do not account for density variations (and hence concentration gradients). At low velocity and high concentration the formation of "plugs" in pipes has been observed and this condition is often called Bingham plastic flow as a consequence.

These findings with dense sediments posed some interesting questions. If vertical turbulence is suppressed, how are the other components affected? Is the conclusion for free surface flow of a reduced wall shear and friction factor a generality? What role does density play?, i.e., will neutrally buoyant particles also "damp" turbulence? What role would flexibility of the particle introduce? Thus, while the

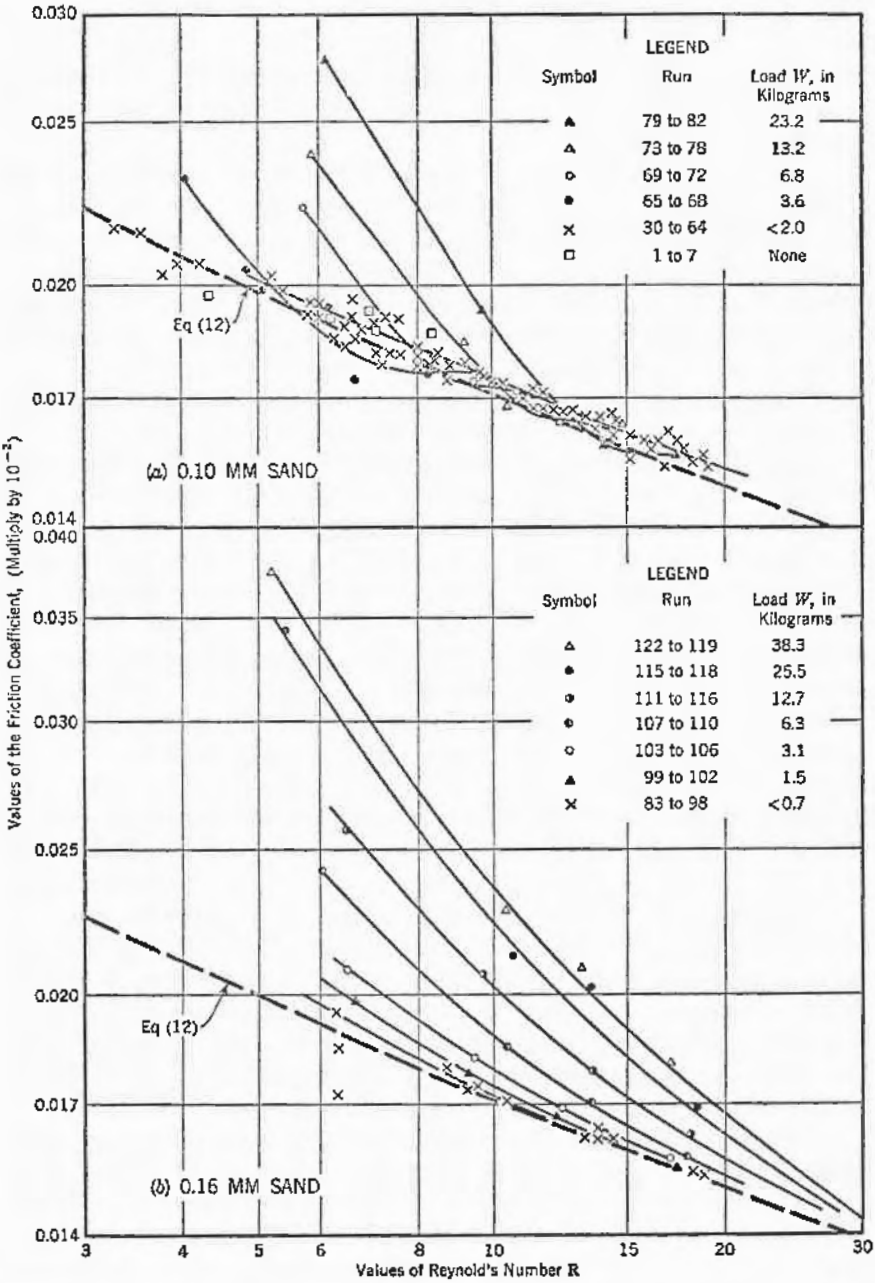

FIG. 6.—FRICTION FACTOR VS. REYNOLDS NUMBER—OPEN CHANNEL WITH FINE SEDIMENT (REF. 2).

findings for suspensions under a strong gravity influence have not been superseded to date, there are currently several investigations looking into the above questions which impinge on the conclusions and explanations offered for these dense particle suspensions. Two areas are suspensions of fibers and suspensions of nearly neutrally buoyant rigid particles.

Experiments with Fiber Suspensions

A suspension of great importance is that composed of paper pulp fibers. Fiber flexibility and its tendency to intermingle and entangle with its neighbors complicates the flow mechanics. On the other hand, the specific gravity of fibers is much smaller than for sands and the gravity effects are correspondingly reduced. The addition of fibers to water produces the effects shown in Fig. 7 where the friction factor f is plotted versus Reynolds number based on the water viscosity. First, it will be noted that extremely large effects are obtained with small concentrations of fibers (1% or less by weight). Second, for any one concentration two regimes are found. At low flows the relation between f

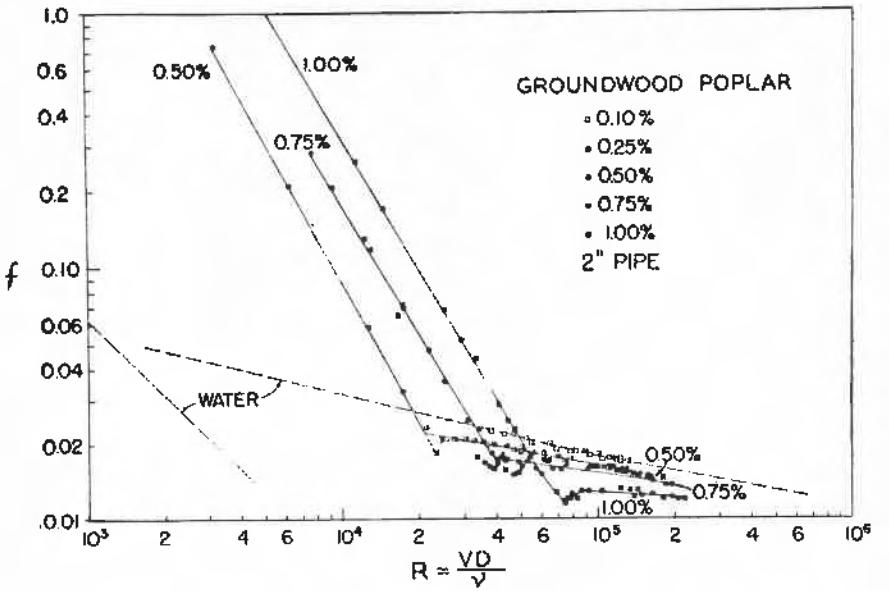

FIG. 7.—FRICTION FACTOR VS. REYNOLDS NUMBER—GROUNDWOOD FIBERS IN A 2" PIPE (REF. 3).

and Reynolds number is "laminar." Visual observations show the solid material to move as a "plug" of entangled fibers surrounded by a clear water zone. Experiments and computations agree with the concept of the entire shear taking place in this clear water annulus as a Couette flow.

This plug flow is conveniently modelled by the Bingham plastic velocity profile. Over the central region of the pipe the velocity is essentially constant. Near the wall the velocity drops steeply. The wall shear, however, is not as conveniently modelled by the Bingham plastic relation as by the Couette model.

The laminar plug flow regime persists to much higher Reynolds numbers than the normal Newtonian fluid flow. The initially high f values drop as Reynolds number increases to a value below the Newtonian turbulent flow friction factor. At this point there is a transition to turbulence and the plug begins to break up. With further increases in Reynolds number the turbulence becomes more intense and more general. At very high Reynolds number the Newtonian friction factor is approached. Apparently, the turbulent forces are so high at high Reynolds numbers that the mixing and shear transmission is completely controlled by turbulence and the factors of fiber interaction and entanglement are unimportant in the process. Hence, the behavior becomes Newtonian although over most of the flow range the behavior is non-Newtonian.

At some flow rates the friction factor, and hence the wall drag, is reduced by as much as 40% with only a 1% addition of fibers. This has been observed also with some liquids having long molecules and has given rise to serious investigations into the possibility of reducing drag of bodies by injecting foreign matter into the boundary layer.

Fig. 8 shows dimensionless velocity profiles with fibers. With increasing concentration the profile becomes blunter. These profiles can be modelled approximately by the power law relation of Eq. (3) by empirically fitting values of n. Since they are all blunter than the Newtonian, $n < 1$ and the behavior is analogous to the pseudoplastic.

The profiles in Fig. 8 present a seeming paradox. They suggest high velocity gradients and hence high shear at the wall. Yet they are for flows where the measured shear and friction factor are definitely lower than Newtonian. The explanation seems to lie in the structure of the turbulent field when fibers are introduced. Fig. 9 shows measurements of u′-turbulent energy versus frequency of turbulent fluctuations.

The area under the curves is the intensity of turbulence (ignore the high peak near 150 cps for Groundwood which is a spurious instrument resonance effect). Note that in general the bulk of the turbulence energy is at low frequencies which correspond to large turbulent eddies. The curves compare water and two different fiber suspensions. They

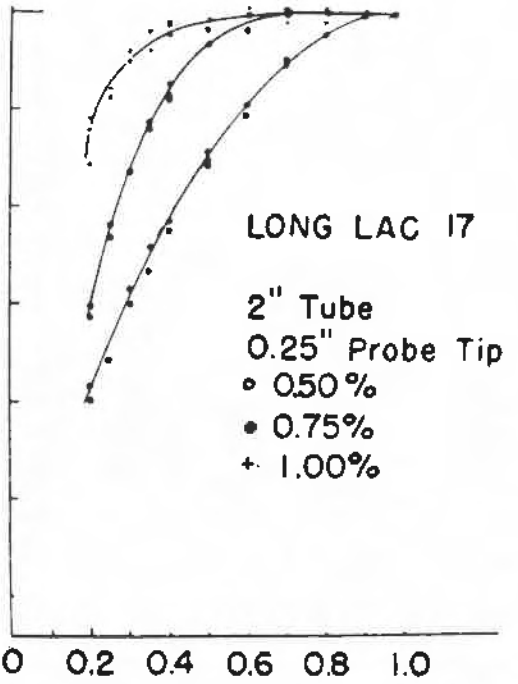

FIG. 8.—DIMENSIONLESS VELOCITY PROFILES—KRAFT SOFTWOOD FIBERS IN A 2" PIPE (REF. 3).

show a reduced intensity and a shift of energy to lower frequencies as fibers are introduced.

The turbulence observations are consistent with the profile and friction factor results if we account for the transmission of momentum (shear) by turbulence and by fiber entanglement and reason (as stated before) that turbulence can break up entangled flows. The mechanism can be described as follows:

Beginning at the wall shear is transmitted primarily by laminar viscous action. In the center of the pipe fiber entanglement predomi-

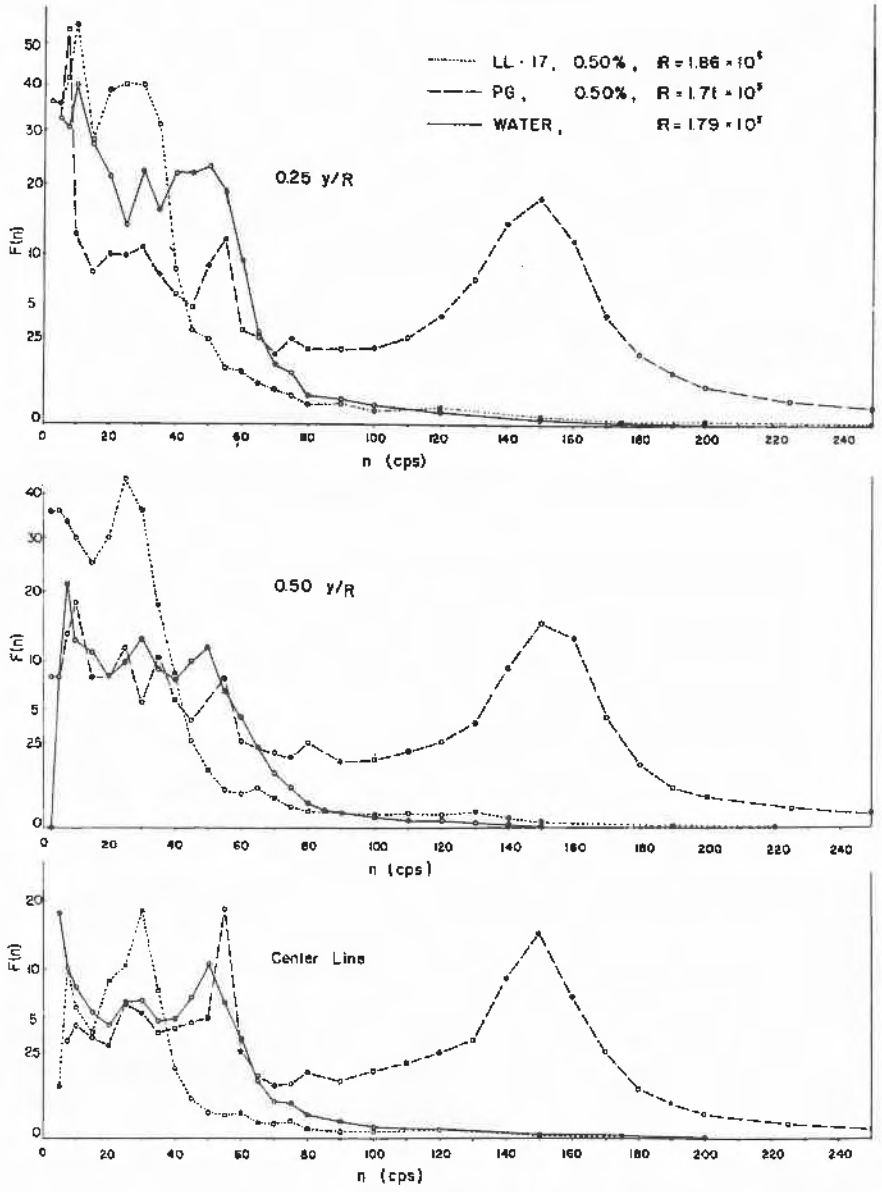

FIG. 9.—U'—TURBULENT ENERGY SPECTRA—WATER AND PAPER PULP FIBERS IN A 2" PIPE (REF. 4).

nates and leads to blunt profiles. Near the wall but outside the laminar sublayer turbulence remains important in breaking up the clusters. Thus, although the turbulence level is reduced from its Newtonian value, it remains the control in the transmission of shear between wall and center. Turbulence is not intense enough to eliminate clusters and control shear transmission in the central portion of the flow. The reduced wall shear, reduced turbulence and the unbroken cluster in the central region represent a balance of conditions.

Rigid Particles in Gravity-Free Suspensions

The findings with high specific gravity sediments and with flexible fibers add importance to the study of the basic question of what a displacement of a fluid volume with a rigid neutrally buoyant particle does to the flow mechanisms.

Bagnold (9) investigated concentrations of large (0.13 cm) neutrally buoyant spherical particles in the turbulent Couette shear flow between a rotating and a stationary cylinder. He measured increases in shear stress over Newtonian values. As an explanation he postulated that due to a particle collision an extra internal stress exists. This stress has two components, a grain shear stress in the direction of shear and a dispersive pressure perpendicular to the shear plane. He showed empirically that the extra shear could be represented in this Couette flow case as

$$T \propto \sigma (\lambda d)^2 (d\bar{u}/dy)^2 \qquad \text{when } \frac{d\bar{u}}{dy} \text{ is large} \tag{20}$$

or

$$T \propto \lambda^{3/2} \mu \, d\bar{u}/dy \qquad \text{when } \frac{d\bar{u}}{dy} \text{ is small} \tag{21}$$

where

T = extra shear

σ = density of particles

λ = linear concentration $= \dfrac{\text{particle diameter}}{\text{clear space between particles}}$

d = particle diameter

μ = fluid viscosity.

Elata and Ippen (5) used fine ($\approx$ 0.01 cm) spherical plastic parti-

cles of specific gravity 1.05 in two-dimensional turbulent flows in an open channel. They measured velocity profiles (Fig. 10) showing the same trends with increased concentration as Vanoni found with dense sediment particles. However, the relation to wall shear was different. The frictional resistance with the plastic particles was greater than the

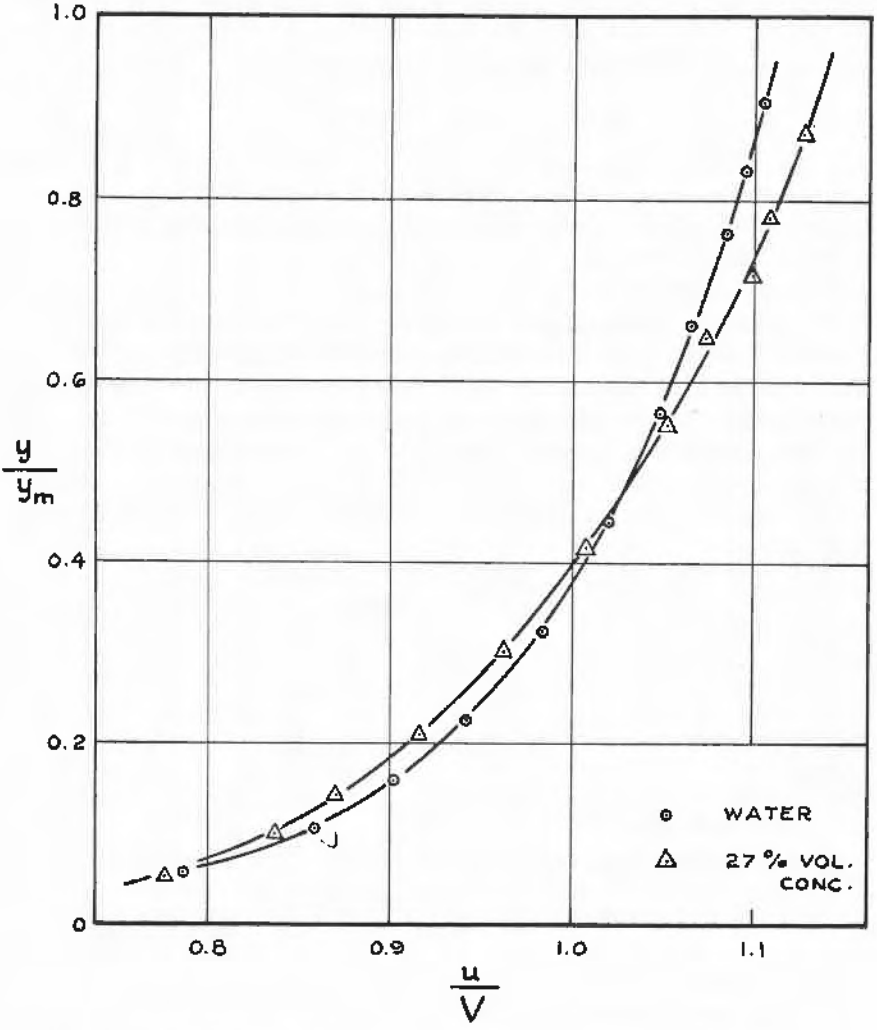

FIG. 10.—DIMENSIONLESS VELOCITY PROFILES—OPEN CHANNEL FLOW WITH FINE NEARLY NEUTRALLY BUOYANT PARTICLES (REF. 5).

Newtonian resistance rather than smaller as Vanoni found. Measurements were made also of the u'-turbulence intensities and found to be higher than for clear water under the same flow conditions. It was concluded that suspensions change the structure of turbulence rather than simply damping the turbulent energy. It was also concluded that the *direct* effect of suspended particles occurs in a narrow zone near the boundary where particles seem to effect an increase in rate of turbulence production.

Fig. 11 shows the friction factor for coarse particles (average diameter = 0.14 cm) of specific gravity 1.035 as determined by Daily

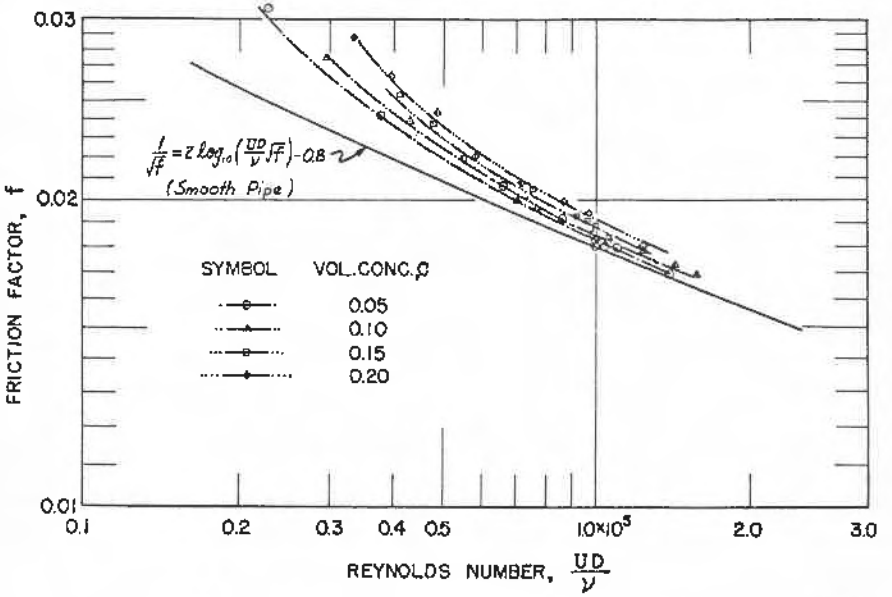

FIG. 11.—FRICTION FACTOR VS. REYNOLDS NUMBER—COARSE NEARLY NEUTRALLY BUOYANT PARTICLES (REF. 6).

and Chu (6) in a 2″-pipe. These also show the friction factor f to increase with concentration above the Newtonian value. At low Reynolds numbers there is settling of the spheres and the resistance rises sharply. Fig. 12 shows dimensionless velocity profiles compared with a profile for water. It is seen that only a small effect of particles is present. The profiles for the suspensions tend to be slightly fuller. A semi-empirical development using an integranual collisional stress

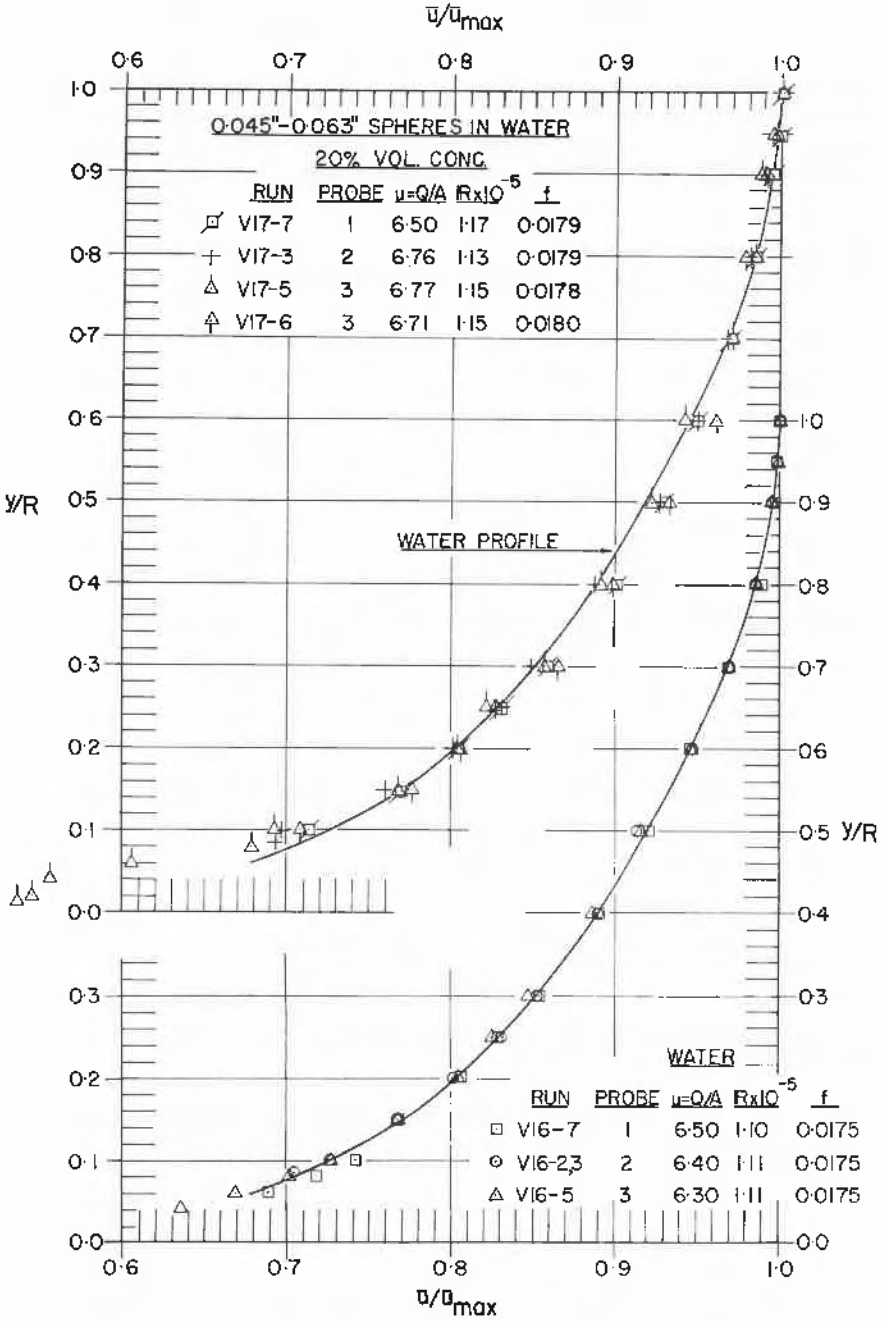

FIG. 12.—DIMENSIONLESS VELOCITY PROFILES—COARSE NEARLY NEUTRALLY BUOYANT PARTICLES IN A 2" PIPE.

concept similar to Bagnold's predicts fuller velocity profiles and higher friction factors as follows:

$$\frac{\bar{u}_{max} - \bar{u}}{u_*} = \frac{1}{k} \ln \frac{R}{y} - \frac{1}{4k} \left(\frac{m\lambda d}{kR}\right)^2 \left[1 - \left(\frac{y}{R}\right)^2\right] + \frac{3}{32k} \left(\frac{m\lambda d}{kR}\right)^4 \left[1 - \left(\frac{y}{R}\right)^4\right] - \dots \quad (22)$$

$$\frac{1}{\sqrt{f}} = 2 \log_{10} (\mathrm{I\!R} \sqrt{f}) - 0.8 - \alpha^2 \left(\frac{m\lambda d}{kR}\right)^2 \quad (23)$$

where in addition to terms previously defined

m = empirical constant
d = particle diameter
R = pipe radius = $D/2$
$\mathrm{I\!R}$ = UD/ν with $U = Q/A$

After correcting the impact probe readings for the effect of the finite probe size, agreement with the experimental results is good if $k = 0.3$, $m = 1.80$ and $\alpha = 1.03$.

Fig. 13 compares profiles for these coarse particles and for the same fine particles used by Elata and Ippen—both measured in the 2″ pipe. There it is seen that, in contrast with the coarse particles, the fine particles have the same sharper form observed in the open channel. On the other hand, friction factors for the fine particles in the pipe were higher than for clear water (as for the coarse particles and for the fine particles in the open channel). Relations for fine particles equivalent to Eqs. (22) and (23) have not been developed. The reasons for the difference between the two results are currently being studied.

Equation (22) considers the Kármán k to be the same constant applying to Newtonian fluids. The value of $k = 0.3$ applies to the water velocity distribution in the outer region of the profile (in the range of $y/R \approx 0.3$ to 0.9). Alternately of course, the fuller profile can be represented as a change in the constant k. The results for coarse particles show k to increase with concentration rather than decrease as Vanoni found for fine sediment. Fig. 14 shows the same data plotted as dimensionless velocity defect profiles. The fuller profile of the coarse particles results in a smaller defect (as predicted by Eq. (22) so long as $\left(\frac{m\lambda d}{kR}\right)$ is less than 1.0). The sharper fine-particle profile gives a larger

defect. It should be noted here that the laminar semi-log relation of Kármán and Prandtl [Eq. (17)] does not describe pipe flow velocity profiles exactly unless $k = k(y)$ even for Newtonian fluids—however, if k is measured always at the same y/R, consistent values are obtained.

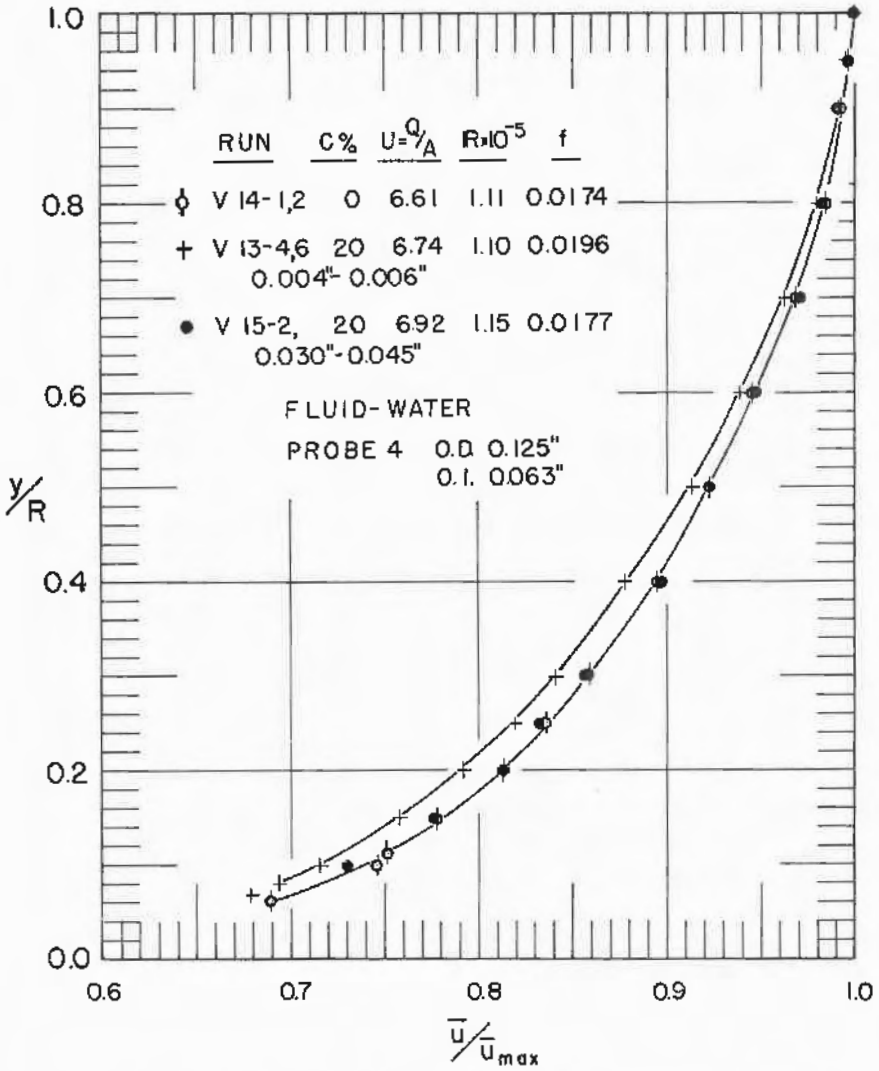

FIG. 13.—DIMENSIONLESS VELOCITY PROFILES—COARSE AND FINE NEARLY NEUTRALLY BUOYANT PARTICLES IN A 2" PIPE.

Figs. 15 and 16 show u′-turbulence spectra and intensities for coarse particles. In Figure 15 the significant data is below about 50 cps. By extrapolation to 1 cps we see that the energy reduction between 1 and 50 cps is in the ratio of 1:20 or 1:25. Thus, the bulk of the turbulent energy is at very low frequencies.

Both Figs. 15 and 16 show significantly higher u′-intensities with suspensions than for water. These increases are considerably higher than the measured increased in shear stress. It is believed that particles in the flow interfere with small turbulent eddies of size comparable to the sphere diameters. On the other hand, rotation and slip of the

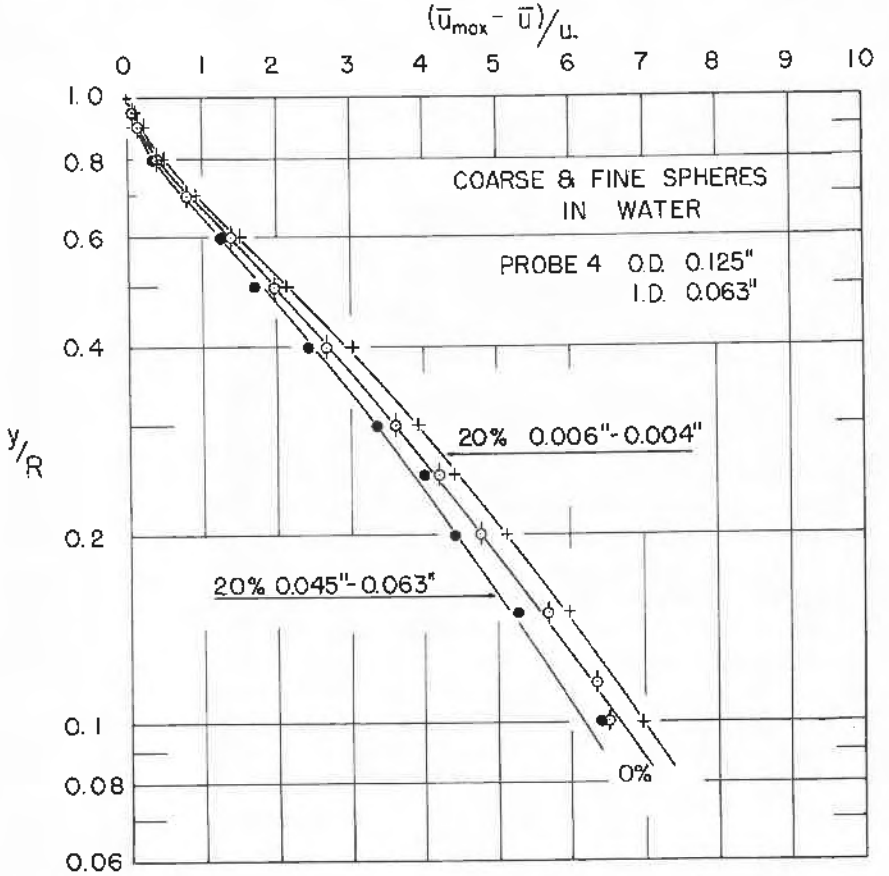

FIG. 14.—DIMENSIONLESS VELOCITY DEFECT—COARSE AND FINE NEARLY NEUTRALLY BUOYANT PARTICLES IN A 2" PIPE (REF. 6).

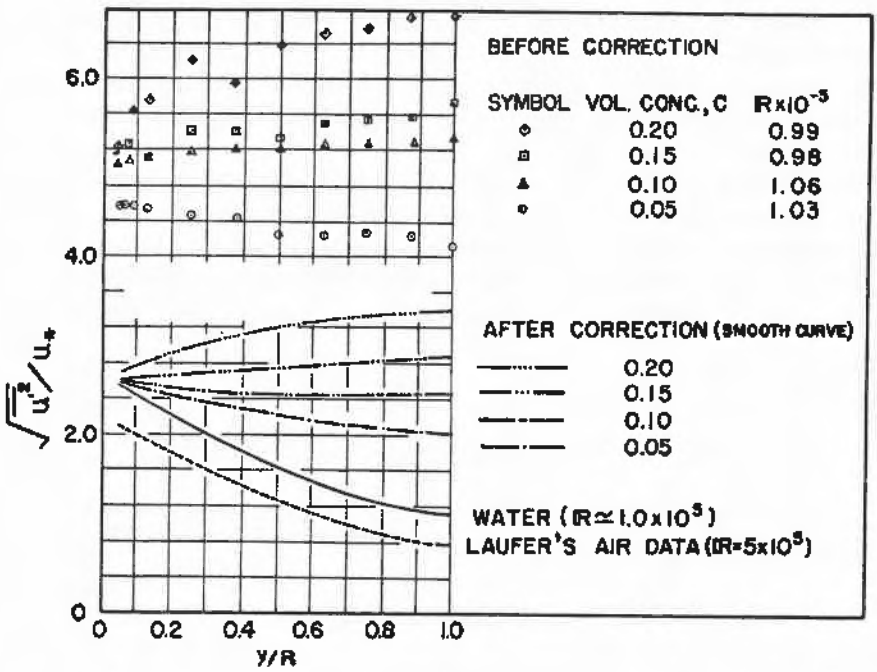

FIG. 15.—U'—TURBULENCE ENERGY SPECTRA—COARSE NEARLY NEUTRALLY BUOYANT PARTICLES IN A 2" PIPE (REF. 6).

particles also give rise to boundary layer development on each sphere and to separation with turbulence generation. Such turbulence probably contributes principally to the high frequency range (small scale eddies). As such its contribution to lateral mixing and momentum transfer (shear stress) may not be in proportion to the increased intensity. Moreover, we should note that basically the turbulent shear stress is the result of a definite correlation between u' and v' components. This is expressed by the mean of their product being finite, or

$$\tau = -\rho\,\overline{u'v'} \neq 0$$

It is concluded that as the u'-turbulence increases, the other components may or may not increase and may or may not maintain the same correlation to the u'-component.

CLOSURE

This has been a summary of the status of the dynamics of three related examples of solid particle suspensions. Sand sediments represent

high specific gravity particles strongly influenced by gravity. Paper pulp fibers represent highly flexible particles with irregular surfaces for which gravity effects are small at high Reynolds numbers. Neutrally buoyant spheres represent a class in which the major effects

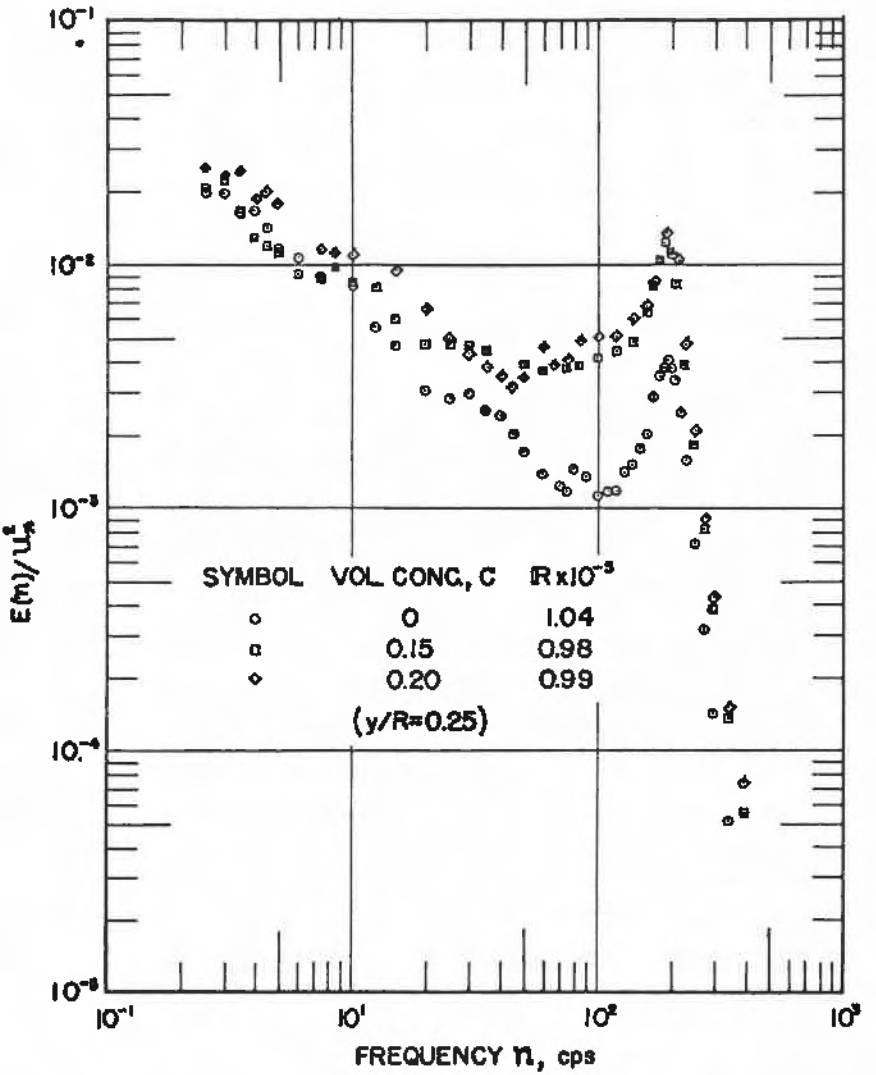

FIG. 16.—U'—TURBULENCE INTENSITIES—COARSE NEARLY NEUTRALLY BUOYANT PARTICLES IN A 2" PIPE (REF. 6).

of the first two are absent. The differences and similarities in behavior indicate a good deal about the relative roles of the three effects although a complete and unifying explanation and theoretical formulation is not yet available. Further investigations are under way for this purpose.

References

1. Vanoni, V. A. "Transportation of Suspended Sediment by Water." Trans. ASCE 111, p. 67 (1946).
2. Ismail, H. M. "Turbulent Transfer Mechanism and Suspended Sediment in Closed Channels." Trans. ASCE 117, p. 409 (1952).
3. Daily, J. W. and Bugliarello, G. "Basic Data for Dilute Fiber Suspensions in Uniform Flow with Shear." TAPPI, Vol. 44, No. 7, July 1961, p. 497.
4. Daily, J. W., Bugliarello, G. and Troutman, W. W. "Measurement and Analysis of Turbulent Flow of Wood Pulp Fiber Suspensions." T.R. No. 35, MIT Civil Engineering Hydrodynamics Laboratory, Sept. 1959.
5. Elata, C. and Ippen, A. T. "The Dynamics of Open Channel Flow with Suspensions of Neutrally Buoyant Particles." T.R. No. 45, MIT Civil Engineering Hydrodynamics Laboratory, Jan. 1961.
6. Daily, J. W. and Chu, T. K. "Rigid Particle Suspensions in Turbulent Shear Flow: Some Concentration Effects." T.R. No. 48, MIT Civil Engineering Hydrodynamics Laboratory, Oct. 1961.
7. Einstein, A. "Eine neue Bestimmung der Moleküldimensionen." Ann. Phys., 19, p. 289 (1906); Berichtigung zu meiner Arbeit "Eine neue Bestimmung der Moleküldimensionen," 34, p. 591 (1911).
8. Eilers, H. "Die Viskosität von Emulsionen hochviskoser Stoffe als Funktion der Konzentrazionen." Kolloid, Z., 97, p. 313 (1941).
9. Bagnold, R. A. "Experiments in a Gravity Free Dispersion of Large Solid Spheres in a Newtonian Fluid under Shear." Proc. Roy. Soc. A 225, p. 49 (1954).